

A model for TRIP steel constitutive behavior

E.S. Perdahcioğlu* and H.J.M. Geijselaers†

*M2i Materials innovation institute, POBox 5008, 2600 GA Delft

†Universiteit Twente, POBox 217, 7500AE Enschede, The Netherlands

Abstract. A constitutive model is developed for TRIP steel. This is a type of steel which contains three or four different phases in its microstructure. One of the phases in TRIP steels is metastable austenite (Retained Austenite) which transforms to martensite upon deformation. The accompanying transformation strain and the increase in hardness provide excellent formability characteristics. The phase transformation depends on the stress in the austenite, which is not equal to the overall stress. An estimate of the local stress in the austenite is obtained by homogenization of the response of the phases using a Mean-Field homogenization method. Overall stress strain results as well as stress strain results for individual phases are compared to measurements found in literature. The model can be used in finite element simulations of forming processes.

Keywords: TRIP, Martensitic transformation, Mean field homogenization

PACS: 81.30.Kf; 62.20.fg

INTRODUCTION

The existence of different phases in the microstructure of TRIP steels is a consequence of its chemical composition and the heat treatment during production. Two main constituent phases are ferrite and austenite and depending on the heat treatment bainite and martensite may also form. The austenite phase (γ) is in a metastable state. It can transform into stable martensite (α') during deformation. One of the attractive features of these steels is the fact that with slight changes in the heat treatment and/or chemical composition, a material with significantly different mechanical properties can be obtained. The aim of this study therefore is to build a model that can be used to predict the final mechanical properties based on the knowledge about the constituent phases.

The model is based on the Mean Field homogenization technique for computing the stress-strain distribution into different phases [1]. In this method the fields for the mechanical variables such as strain and stress are represented by their average values over the sub-domains. This method is well established to be used for binary mixtures of phases. Extension to mixtures of three or four phases have been presented in [2, 3]. Also in this research application of this method for more than two phases is investigated. One of the possibilities is to use the self-consistent scheme that implicitly takes into account existence of any number of phases. The drawback however with this method is that it is computationally intensive. Therefore another scheme is proposed that is much more efficient and comparable in accuracy to the self-consistent method. This model can be used in finite element simulations of forming processes.

The martensitic transformation is modeled as a stress-driven process [4, 5, 6]. This is in contrast to the model of deformation induced martensitic transformation [7, 8]. The model depends on the stress resolved in the austenite phase and transformation is determined as a function of the additional mechanical driving force supplied to the material [9, 10].

MEAN FIELD HOMOGENIZATION

The Mean-Field method is based on the interaction and evolution of the average values of the field variables in sub-domains that divide the overall structure. The overall stress $\boldsymbol{\sigma}$ and strain $\boldsymbol{\varepsilon}$ are related to those in the individual phases by

$$\boldsymbol{\sigma} = \sum f_i \boldsymbol{\sigma}_i, \quad \boldsymbol{\varepsilon} = \sum f_i \boldsymbol{\varepsilon}_i \quad (1)$$

The f_i stands for the volume fraction of the phases ferrite, bainite, austenite and martensite. It is assumed that the macroscopic stress-strain relation that is determined for an individual phase is also valid within the compound.

$$\dot{\boldsymbol{\sigma}}_i = \mathbb{C}_i : \mathbf{D}_i \quad (2)$$

where \mathbf{D}_i is the strain rate in the i^{th} phase and \mathbb{C}_i is an elasto-plastic material tangent. For closure also the relations between phase strains and overall strain must be specified:

$$\mathbf{D}_i = \mathbb{A}_i : \mathbf{D} \quad (3)$$

The fourth order tensor \mathbb{A}_i is the strain concentration tensor which is subject to:

$$\sum f_i \mathbb{A}_i = \mathbb{I} \quad (4)$$

where \mathbb{I} is the fourth order unit tensor. The homogenized response can then be calculated as:

$$\mathbb{C} = \sum f_i \mathbb{C}_i : \mathbb{A}_i \quad (5)$$

Different homogenization schemes have been derived depending on a specific definition of \mathbb{A} . The most common schemes that can also be used for more than two phases are Voigt (iso-strain), Reuss (iso-stress) and self-consistent.

simple bounds

In the Voigt-Taylor scheme the strain in each phase is assumed equal to the overall strain: $\mathbb{A}_i = \mathbb{I}$. Then the homogenized response is found as: $\mathbb{C} = \sum f_i \mathbb{C}_i$. In the Reuss-Sachs scheme on the other hand the phase stresses are assumed equal. The strain concentration tensor can then be derived to be $\mathbb{A}_i = \mathbb{C}^{-1} : \mathbb{C}_i$ and the overall response is $\mathbb{C} = (\sum f_i \mathbb{C}_i^{-1})^{-1}$. The responses of the Voigt and the Reuss models constitute upper and lower bounds to the stiffness of the response of the actual system. It is clear that these schemes are explicit.

self-consistent

The self-consistent scheme has originally been developed to compute the mechanical response of polycrystals [11, 12, 13] where the interaction of the matrix and the individual grains is taken into account using Eshelby's equivalent inclusion theory [14]. In the self-consistent scheme each phase is considered as an inclusion in a matrix which has homogenized response. The strain concentration tensor for phase i is defined as:

$$\mathbb{A}_i = (\mathbb{I} + \mathbb{S} : (\mathbb{C}^{-1} : \mathbb{C}_i - \mathbb{I}))^{-1} \quad (6)$$

where \mathbb{S} is the fourth order Eshelby tensor [14, 15] and \mathbb{C} is the overall response as defined by (5). The Eshelby tensor also depends on \mathbb{C} . This is a scheme which is implicit, meaning that determination of \mathbb{A}_i requires an iterative procedure. This makes that application of the self-consistent scheme in full scale finite element calculations is not very attractive.

interpolation between bounds

Here another algorithm is proposed where the strain concentration is defined as an interpolation between the Voigt and Reuss schemes. For the proposed strain concentration tensor first the interpolation is defined as:

$$\mathbb{H}_i = \left(\varphi_i \mathbb{I} + (1 - \varphi_i) (\sum f_j \mathbb{C}_j^{-1}) : \mathbb{C}_i \right) \quad (7)$$

Next, to assure that the sum of \mathbb{A}_i yields unity as in (4), the strain concentration for each phase is defined by:

$$\mathbb{A}_i = \mathbb{H}_i : (\sum f_j \mathbb{H}_j)^{-1} \quad (8)$$

The interpolation function $\varphi_i = \varphi(f_i)$ is chosen such that the overall response as well as the strain concentrated in each phase closely match the results obtained with the self-consistent approach. Satisfactory results are obtained with $\varphi(f) = 0.5 + 0.3f$.

TRANSFORMATION OF RETAINED AUSTENITE

The transformation of the retained austenite is modeled using an algorithm previously developed for metastable austenitic stainless steels in which the main driving factor is the stress resolved in the austenite phase.

$$f_{\alpha'} = f_{\alpha'}^0 + F(U^{\max} - \Delta G^{\text{cr}}) * f_{\gamma}^0 \quad (9)$$

Here U^{\max} is the supplied driving force [9, 10, 16, 17] and is a function of the stress in the austenite phase σ_{γ} and the transformation strain during martensite transformation. $f_{\alpha'}^0$ and f_{γ}^0 are the initial phase fractions of martensite and austenite. ΔG^{cr} is the critical energy barrier which is experimentally determined. The function F resembles a saturating exponential curve as in [18] with smoothed transitions [17]. The supplied driving force is calculated by:

$$U^{\max} = \sum \lambda_i \sigma_{\gamma_i} \quad (10)$$

where σ_{γ} are the ordered principal stresses in the austenite and λ are the ordered eigenvalues of the transformation strain accompanying the martensite transformation.

$$\lambda = \text{eig} \left(\frac{1}{2} (\mathbf{d} \otimes \mathbf{n} + \mathbf{n} \otimes \mathbf{d}) \right) \quad (11)$$

Here \mathbf{n} and \mathbf{d} are the habit plane normal and the shear displacement for a martensitic variant. In terms of the often quoted transformation dilatation $\delta = \mathbf{n} \cdot \mathbf{d}$ and shear $\gamma = (\mathbf{1} - \mathbf{n} \otimes \mathbf{n}) \cdot \mathbf{d}$ the values of λ can be easily calculated as:

$$\lambda_{1,3} = \frac{1}{2} \left(\delta \mp \sqrt{\gamma^2 + \delta^2} \right), \quad \lambda_2 = 0 \quad (12)$$

U^{\max} in (10) is equivalent to the expression for U_{\max} in [16] generalized to arbitrary stress states.

CONSTITUTIVE MODEL

The strain rate is partitioned in a transformation plasticity and the elastoplastic strain rate. The latter is partitioned among the phases.

$$\mathbf{D} = \mathbf{D}^{\text{ep}} + \mathbf{D}^{\text{tp}} = \sum f_i \mathbf{D}_i + \mathbf{D}^{\text{tp}} \quad (13)$$

The resulting stress response is then:

$$\dot{\boldsymbol{\sigma}} = \sum f_i \dot{\boldsymbol{\sigma}}_i = \left(\sum f_i \mathbb{C}_i : \mathbb{A}_i \right) : (\mathbf{D} - \mathbf{D}^{\text{tp}}) \quad (14)$$

The transformation plasticity is calculated according to [17, 19]. A transformation plasticity is assumed as:

$$\mathbf{D}^{\text{tp}} = \dot{f}_{\alpha'} \left(\frac{3}{2} T \mathbf{s}_{\gamma} + \frac{1}{3} \delta \mathbf{1} \right) \quad (15)$$

where \mathbf{s}_{γ} is the deviatoric stress in the austenite phase and $\mathbf{1}$ is the second order unit tensor. T is the amount of shape change and can be calculated from the assumption that the product of the current austenite stress and the transformation plasticity strain is always equal to ΔG^{cr} :

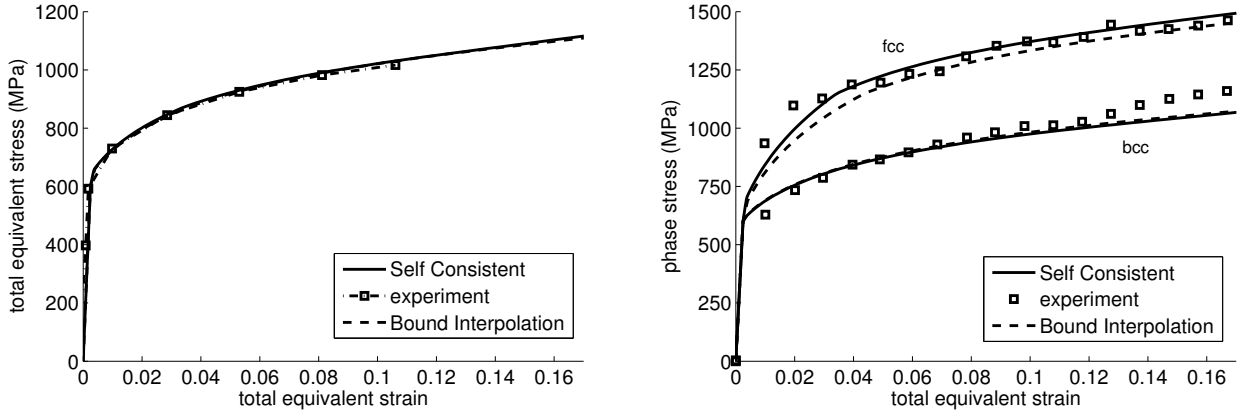
$$T(\boldsymbol{\sigma}_{\gamma}) = \frac{1}{(\sigma_{\gamma}^{\text{vM}})^2} \left(\Delta G^{\text{cr}} - \sigma_{\gamma}^{\text{h}} \delta \right) \quad (16)$$

where $\sigma_{\gamma}^{\text{vM}}$ is the von Mises equivalent stress and $\sigma_{\gamma}^{\text{h}}$ is the hydrostatic stress component in the austenite phase. For TRIP steel with low initial austenite fraction the contribution of the transformation plasticity is very small however.

TABLE 1. Material data of different phases used for simulation of TRIP steel

Phase	fraction	E (GPa)	ν	σ_0^y (MPa)	K (MPa)	m	ϵ^0
martensite	0*	210	0.3	1500	1000	0.12	0.001
austenite	0.12*	210	0.3	1150	1500	0.21	0.010
bainite	0.33	210	0.3	700	1000	0.19	0.008
ferrite	0.55	210	0.3	600	1500	0.19	0.008

*initial

**FIGURE 1.** a) Overall stress as a function of overall strain, b) Stress in the phases as a function of overall strain

SIMULATIONS

In [20] extensive stress and strain measurements on a specific TRIP steel are presented. The strain partitioning among the phases was measured by digital image correlation on SEM micrographs acquired in situ during tensile tests. The stress partitioning between the phases was measured by neutron diffraction in situ during tensile tests. The elastic strains of the fcc phase (austenite) and the bcc phases ferrite and bainite could be measured. Stresses in individual bcc phases can not be obtained since all give identical diffraction peaks.

The stress strain response of this TRIP steel has been simulated with the self-consistent method as well as with the bound interpolation method. The steel consists of four phases: ferrite, bainite, austenite and martensite. The material data used to simulate the response are given in table 1.

The yield stress is described by the hardening function $\sigma_i^y(\epsilon_i^p) = \sigma_i^0 + K_i(\epsilon_i^0 + \epsilon_i^p)^m$.

The critical energy barrier for transformation is chosen as $\Delta G^{cr} = 175\text{MPa}$.

The transformation strain is characterized by $\delta = 0.02$ and $\gamma = 0.23$.

In Figure 1a the computed response of the TRIP steel loaded under uniaxial tension is shown. The simulations both with the self-consistent method and the bound interpolation method agree well with the experimental data from [20]. The partitioning of the stress among the fcc and bcc phases is shown in Figure 1b. The stress in the bcc phase is the average stress in ferrite and bainite. In Figure 2 the evolution of the retained austenite fraction is shown, compared to experimental results. The results are a bit inconclusive. Note however that quantitative measurement of retained austenite is not trivial [21]. The simulation with the self-consistent method uses approximately 10 times more time than that with bound interpolation.

CONCLUSIONS

For multi-phase simulations of TRIP steel the self-consistent scheme was implemented. It was found that although it is possible to use this scheme for this purpose, it is very inefficient to be used in a full scale simulation. A new scheme for multi-phase materials is proposed and has been generalized and implemented. It is seen that the new scheme is much more efficient and its results compare well with those of the self-consistent model.

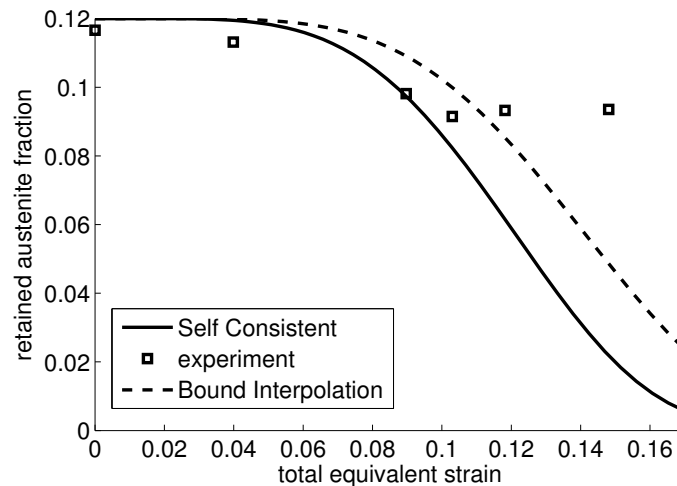


FIGURE 2. Fraction retained austenite as a function of overall strain

The homogenization scheme has been complemented with a model for martensitic transformation. The stress in the austenite is assumed to be the main factor that determines the transformation.

The results of simulations compare well with measurements in literature when stress partitioning and overall response are considered.

ACKNOWLEDGMENTS

This research was carried out under project number M63.1.09373 in the framework of the Research Program of the Materials innovation institute M2i (www.m2i.nl).

REFERENCES

1. I. Doghri, and C. Friebe, *Mechanics of Materials* **37**, 45–68 (2005).
2. F. Lani, Q. Furnémont, T. V. Rompaey, F. Delannay, P. J. Jacques, and T. Pardoen, *Acta Materialia* **55**, 3695–3705 (2007).
3. L. Delannay, P. J. Jacques, and T. Pardoen, *International Journal of Solids and Structures* **45**, 1825–1843 (2008).
4. I. Tamura, *Metals Science* **16**, 245–254 (1982).
5. S. Chatterjee, and H. K. D. H. Bhadeshia, *Materials Science and Technology* **23**, 1101–1104 (2007).
6. A. Das, P. C. Chakraborti, S. Tarafder, and H. K. D. H. Bhadeshia, *Materials Science and Technology* **27**, 366–370 (2011).
7. G. B. Olson, and M. Cohen, *Metallurgical Transactions A* **6**, 791–795 (1975).
8. R. G. Stringfellow, D. M. Parks, and G. B. Olson, *Acta Metallurgica & Materialia* **40**, 1703–1716 (1992).
9. F. D. Fischer, and G. Reisner, *Acta Metallurgica* **46**, 2095–2102 (1998).
10. H. J. M. Geijselaers, and E. S. Perdahcioğlu, *Scripta Materialia* **60**, 29–31 (2009).
11. E. Kröner, *Zeitschrift der Physik* **151**, 504–518 (1958).
12. B. Budiansky, and T. T. Wu, “Theoretical Prediction of Plastic Strains of Polycrystals,” in *Proc. 4th US Natl. Congr. Appl. Mech. ASME*, 1962, pp. 1175–1185.
13. R. Hill, *Journal of Mechanics and Physics of Solids* **13**, 213–222 (1965).
14. J. D. Eshelby, *Proc. of the Royal Society of London* **A241**, 376–396 (1957).
15. T. Mura, *Micromechanics of Defects in Solids*, Martinus Nijhoff Publishers, 1982.
16. J. R. Patel, and M. Cohen, *Acta Metallurgica* **1**, 531–538 (1953).
17. E. S. Perdahcioğlu, *Constitutive modeling of metastable austenitic stainless steel*, Ph.D. thesis, Universiteit Twente (2008).
18. D. P. Koistinen, and R. E. Marburger, *Acta Metall.* **7**, 59–60 (1959).
19. C. L. Magee, *Transformation Kinetics, Microplasticity and Aging of Martensite in Fe-31 Ni*, Ph.D. thesis, Carnegie Institute of Technology (1966).
20. P. J. Jacques, Q. Furnémont, F. Lani, T. Pardoen, and F. Delannay, *Acta Materialia* **55**, 3681–3693 (2007).
21. P. J. Jacques, S. Allain, O. Bouaziz, A. De, A.-F. Gourgues, B. M. Hance, Y. Houbaert, J. Huang, A. Iza-Mendia, S. Kruger, M. Radu, L. Samek, J. G. Speer, L. Zhao, and S. van der Zwaag, *Materials Science and Technology* **25**, 567–574 (2009).